

Particle-based adaptive-lag online marginal smoothing in general state-space models

Johan Alenlöv and Jimmy Olsson

Abstract—We present a novel algorithm, an adaptive-lag smoother, approximating efficiently, in an online fashion, sequences of expectations under the marginal smoothing distributions in general state-space models. The algorithm evolves recursively a bank of estimators, one for each marginal, in resemblance with the so-called particle-based, rapid incremental smoother (PaRIS). Each estimator is propagated until a stopping criterion, measuring the fluctuations of the estimates, is met. The presented algorithm is furnished with theoretical results describing its asymptotic limit and memory usage.

Index Terms—Sequential Monte Carlo methods, state-space models, marginal smoothing, PaRIS, particle filters, state estimation.

I. INTRODUCTION

STATE-SPACE models (SSMs), also known as *hidden Markov models* (HMMs), are fundamental in many scientific and engineering disciplines. Incorporating unobservable, Markovian states, these models are adjustable enough to model a variety of complex, real-world time series in, e.g., econometrics [6], speech recognition [32], and target tracking [24]. In this paper we focus on online state reconstruction in SSMs; more specifically, our goal is to estimate, on-the-fly as new data appear, expectations under the marginal posteriors of the different states given the data.

More precisely, an SSM is a bivariate model consisting of an observable process $\{Y_t\}_{t \in \mathbb{N}}$, referred to as the *observation process*, and an unobservable Markov chain $\{X_t\}_{t \in \mathbb{N}}$, known as the *state process*, taking on values in some general measurable spaces (Y, \mathcal{Y}) and (X, \mathcal{X}) , respectively. Throughout the paper the subindex t will often be referred to as “time” without being necessarily a temporal index.

When operating on SSMs one is often interested in calculating expectations under the conditional distribution of one or several states conditioned upon a subset of some given stream $\{y_t\}_{t \in \mathbb{N}}$ of observations. For any $(s, s', t) \in \mathbb{N}^3$ such that $s \leq s' \leq t$ we denote by $\phi_{s:s'|t}$ the conditional distribution of $X_{s:s'} = (X_s, \dots, X_{s'})$ (our notation for vectors) given $Y_{0:t} = y_{0:t}$ (a precise definition is given in Section II). Some special distributions of interest are the *filter distributions* $\phi_t := \phi_{t:t|t}$, the *joint smoothing distributions* $\phi_{0:t|t}$, and, finally, when $s = s'$, the *marginal smoothing distributions* $\phi_{s|t}$.

For any probability measure μ and real-valued measurable function h , let $\mu h := \int h(x) \mu(dx)$ denote the Lebesgue

integral of h with respect to μ (whenever this is well defined). Given an observation stream $\{y_t\}_{t \in \mathbb{N}}$ and a sequence $\{h_t\}_{t \in \mathbb{N}}$ of real-valued functions, the present paper focuses on online calculation of the flow

$$(\phi_{0|t}h_0, \phi_{1|t}h_1, \dots, \phi_{s|t}h_s, \dots, \phi_{t-1|t}h_{t-1}, \phi_t h_t), \quad t \in \mathbb{N}, \quad (1)$$

as t increases. Note that a significant challenge with this problem is that *all* elements of the vector (1) change with t . Moreover, in the problem formulation, the word “online” means, first, that the observation sequence is processed in a single sweep as new observations appear and, second, that the computational cost of updating the approximations one step, i.e., from t to $t + 1$, is uniformly bounded in t . Hence, the aggregated computational cost and memory requirements of the algorithm should grow at most linearly with t .

Remark 1. *In the literature (see, e.g., [3]), the problem of computing $\phi_{s|t}$ offline for a fixed t and all $s \leq t$ is typically referred to as fixed-interval smoothing. On the other hand, the problem of computing $\phi_{s|t}$ online for a fixed s and increasing t is typically referred to as fixed-point smoothing. Our aim of computing the whole vector (1) online could hence be viewed as a combination of these two problems.*

A. Previous work

Exact smoothing is possible only in models with finite state space and for linear Gaussian SSMs using the *forward-backward smoother* [31] and the *disturbance smoother* [7] (sometimes referenced to as the *Kalman smoother*), respectively. When dealing with general, possibly nonlinear SSMs, current methods take mainly two different approaches. The first approach relies, as in the *extended Kalman filter* and the *unscented Kalman filter* [1], [20], on linearisation of the model and Kalman filtering. These methods work well if the model is almost linear Gaussian, but will introduce significant errors in the presence of highly nonlinear model components.

The second approach relies on Monte Carlo simulation, preferably in the form of *sequential Monte Carlo* (SMC) *methods*, or, *particle filters*. Particle filters propagate recursively a sample of random simulations, so-called *particles*, mimicking typically, as in the *bootstrap particle filter*, the latent state (or, prior) dynamics. At each time step, the particles are associated with importance weights compensating for the discrepancy between the prior dynamics and the conditional (posterior) dynamics of the states given the observations. By duplicating and killing, through resampling, particles with high and low importance, respectively, the particles are directed towards regions of the state space with high posterior probability.

J. Alenlöv is with the Department of Information Technology, Uppsala University, Sweden, e-mail: johan.alenlov@it.uu.se

J. Olsson is with the Department of Mathematics, KTH Royal Institute of Technology, Sweden, e-mail: jimmyol@kth.se

At each time step, the weighted empirical measure associated with the particles serves as an approximation of the filter distribution at the time step in question. Moreover, it can be shown that the empirical measure formed by the ancestral lines of the particles provides an approximation also of the joint smoothing distribution. However, since the particles are resampled repeatedly, these trajectories collapse eventually, and in the long run such a Monte Carlo approximation will rely on more or less a single path. Thus, the statistician is referred to alternative techniques such as the *forward-filtering backward-smoothing* (FFBSm) [13], *forward-filtering backward-simulation* (FFBSi) [15] or *joint backward simulation Rao-Blackwellized particle filter* [23] algorithms, which approximate the so-called *backward decomposition* of the joint smoothing distribution. The *two-filter algorithm* [21], [3], [14], [26] combines two separate particle filters, one in the forward direction and one in the reverse direction. In the *adaptive path integral smoother* [33], smoothing is performed by solving a control problem. A popular class of methods are the *Markov chain Monte Carlo* (MCMC) methods simulating a Markov chain admitting the joint smoothing distribution as invariant distribution. Recently, [2] combined successfully particle methods and MCMC into *particle Markov chain Monte Carlo* (PMCMC) methods to construct such Markov chains. All of these methods, in their most basic forms, require more than one pass of the data, either a forward and backward pass or that the estimates needs to be iterated until convergence is reached. Thus, the online processing setting of the present paper invalidates these methods.

As known to us, there is only one existing approach that applies to the problem (1) without violating the online criteria set up by us, namely the particle-based *fixed-lag smoother* [22], [27]. This is a genealogical tracing-based particle method that copes with particle path degeneracy by means of truncation. The truncation implies a bias that may be controlled using forgetting arguments (see [27] for an analysis). A problem with this method, which will be explained in some detail in Section IV-B, is that the truncation lag is a design parameter that needs to be set a priori by the user. This is nontrivial, as the optimal choice of the lag depends on the mixing properties of the model.

B. Our Contribution

In the present paper we introduce a novel algorithm that provides an approximate solution to the research question outlined in the previous section. The algorithm relies on a recursive form of the backward decomposition that has been employed previously for forward smoothing of additive state functionals [4], [10]. The same decomposition is used in the *particle-based, rapid incremental smoother* (PaRIS), proposed by the authors in [28] and analysed theoretically in [29], which performs online smoothing of additive state functionals with constant memory and computational complexity demands that grow only linearly with the number of particles (compared to the quadratic growth of other algorithms [10]).

The method proposed in the present paper is driven by the same sampling technique as the PaRIS and could be likened

to computing one PaRIS estimate per marginal in (1). All these PaRIS estimates are formed on the basis of the output of the same underlying particle filter. However, since our aim is to compute, on-the-fly, *all* the marginal expectations in (1), we need, in order to avoid computational overload, to stop updating the estimate of a given marginal expectation once some criterion tells us to do so. This leads to an *adaptive-lag approach*. A sensible such stopping criterion will be designed using the forgetting properties of the model.

Our contribution is presented in two steps: first, we consider an ideal algorithm, applicable in the context of linear Gaussian models and requiring closed-form computation of all quantities of interest; after this, the general—possible nonlinear/non-Gaussian—case is dealt with using particle-based approximations. By using results derived in [29], we are able to analyse theoretically the asymptotic properties and memory demands of our algorithm in order to place the same on more solid ground.

Finally, we illustrate numerically the performance of the proposed algorithm and compare the same to that of the marginal fixed-lag smoother. As shown by the simulations, our adaptive-lag approach avoids completely the complex bias-variance tradeoff that is an unavoidable ingredient of optimal fixed-lag design. Moreover, it is shown that the marginal adaptive-lag smoother is on par with the optimally tuned fixed-lag smoother in terms of variance.

C. Outline

In Section II we introduce formally SSMs and the backward decomposition. Section III introduces the ideal algorithm, providing a conceptual understanding of our approach without involving particle approximations. In Section IV we turn to the nonlinear/non-Gaussian case and replace intractable quantities by particle-based estimates. Theoretical results are presented in Section V and in Section VI the algorithm is benchmarked numerically on two models. Our conclusions are presented in Section VII and, finally, Section A contains some proofs.

II. PRELIMINARIES

In the following, let \mathbb{N} and \mathbb{N}^* denote the sets of nonnegative and positive natural numbers, respectively. For any bounded measurable function h we let $\|h\|_\infty := \sup_{x \in X} |h(x)|$ and $\text{osc}(h) := \sup_{(x, x') \in X^2} |h(x) - h(x')|$ denote the supremum and oscillator norms of h , respectively.

In the following we assume that all random elements are well-defined on a common probability space $(\Omega, \mathcal{F}, \mathbb{P})$. Let (X, \mathcal{X}) and (Y, \mathcal{Y}) be some measurable spaces, $\mathbf{Q} : X \times \mathcal{X} \rightarrow [0, 1]$ and $\mathbf{G} : X \times \mathcal{Y} \rightarrow [0, 1]$ some Markov transition kernels, and χ a probability measure on \mathcal{X} . An SSM is a bivariate Markov chain $\{(X_t, Y_t)\}_{t \in \mathbb{N}}$ on $X \times Y$ such that $X_{t+1}, Y_{t+1} \mid X_t, Y_t \sim \mathbf{Q}(X_t, dx_{t+1}) \mathbf{G}(x_{t+1}, dy_{t+1})$ and $X_0, Y_0 \sim \chi(dx_0) \mathbf{G}(x_0, dy_0)$. It is assumed that only $\{Y_t\}_{t \in \mathbb{N}}$ is observable. Using this definition, it is easily shown that

- (i) the unobservable state sequence $\{X_t\}_{t \in \mathbb{N}}$ is a Markov chain with transition kernel \mathbf{Q} and initial distribution χ .
- (ii) the variables of the observable process $\{Y_t\}_{t \in \mathbb{N}}$ are, conditionally on the states, independent and such that

the conditional distribution of each Y_t depends on the corresponding X_t only.

Throughout this paper we will assume that the model is *fully dominated*, i.e., that \mathbf{Q} and \mathbf{G} admit transition densities q and g , respectively, with respect to some reference measures. We will in the following assume that we are given a fixed stream $\{y_t\}_{t \in \mathbb{N}}$ of observations. For ease of notation, let for all $t \in \mathbb{N}$, $g_t(x) := g(x, y_t)$, $x \in \mathbf{X}$. The joint smoothing distribution at time t , i.e., the law of $X_{0:t}$ conditionally to $Y_{0:t} = y_{0:t}$, is

$$\phi_{0:t|t}(\mathrm{d}x_{0:t}) := \frac{\chi(\mathrm{d}x_0)g_0(x_0) \prod_{s=1}^t \mathbf{Q}(x_{s-1}, \mathrm{d}x_s)g_s(x_s)}{\int \cdots \int \chi(\mathrm{d}x'_0)g_0(x'_0) \prod_{s=1}^t \mathbf{Q}(x'_{s-1}, \mathrm{d}x'_s)g_s(x'_s)},$$

and all posteriors $\phi_{s:s'|t}$ of interest (including the filter ϕ_t) are obtained as marginals of $\phi_{0:t|t}$.

Interestingly, the state process is still Markov when evolving conditionally to $Y_{0:t}$ in the time-reversed direction; in particular, using Bayes' formula and the Markov property of the bivariate process $\{(X_t, Y_t)\}_{t \in \mathbb{N}}$ it is checked straightforwardly that the distribution of X_s given $X_{s+1} = x_{s+1}$ and $Y_{0:s} = y_{0:s}$ is given by

$$\overleftarrow{\mathbf{Q}}_{\phi_s}(x_{s+1}, \mathrm{d}x_s) := \frac{q(x_s, x_{s+1})\phi_s(\mathrm{d}x_s)}{\int q(x'_s, x_{s+1})\phi_s(\mathrm{d}x'_s)}, \quad s \in \mathbb{N} \quad (2)$$

(see, e.g., [5, Prop. 3.3.6]). Using (2), the joint-smoothing distribution may be expressed by the *backward decomposition*

$$\phi_{0:t|t}(\mathrm{d}x_{0:t}) = \phi_t(\mathrm{d}x_t) \prod_{s=0}^{t-1} \overleftarrow{\mathbf{Q}}_{\phi_s}(x_{s+1}, \mathrm{d}x_s),$$

which is instrumental in many smoothing procedures [15], [11], [29], [10].

III. ONLINE MARGINAL SMOOTHING

Recall that our aim is to estimate the vectors (1) in an online manner as t increases. For the moment, consider estimation of some expectation $\phi_{s|t}h_s$ under some marginal $\phi_{s|t}$. Under suitable ergodicity conditions (to be specified later), we may expect observations of the distant future to have limited effect on the posterior of some state X_s . Consequently, we may expect $\phi_{s|t}h_s$ to converge to some fixed point $\phi_{s|\infty}h_s$ as t increases; see [5, Sec. 4.3]. Thus, allowing for a negligible bias, we may update $\phi_{s|t}h_s$ only as long as the sequence $\{\phi_{s|t}h_s\}_{t=s}^{\infty}$ exhibits discernible fluctuations, i.e., until, say, $t = s_\varepsilon$, and approximate $\phi_{s|t}h_s$ by $\phi_{s|s_\varepsilon}h_s$ for all $t \geq s_\varepsilon$. Here ε is an algorithmic parameter regulating the stopping criterion. This idea is explored in the following.

A. An ideal algorithm

Let $(s, t) \in \mathbb{N}$ be such that $s \leq t$ and consider the marginal expectation $\phi_{s|t}h_s = \mathbb{E}[h_s(X_s) \mid Y_{0:t} = y_{0:t}]$. By the tower property,

$$\mathbb{E}[h_s(X_s) \mid Y_{0:t} = y_{0:t}] = \mathbb{E}[T_{s|t}(X_t) \mid Y_{0:t} = y_{0:t}], \quad (3)$$

where

$$T_{s|t}(x_t) := \mathbb{E}[h_s(X_s) \mid Y_{0:t-1} = y_{0:t-1}, X_t = x_t], \quad x_t \in \mathbf{X}, \quad (4)$$

is a statistic appearing frequently in the literature on smoothing; see for instance [29], [11], [10]. Appealingly, reapplying the tower property, the statistics $\{T_{s|t}\}_{t=s}^{\infty}$ can be expressed recursively (see [25], [4], [9]) through

$$\begin{aligned} T_{s|t+1}(x_{t+1}) &= \mathbb{E}[T_{s|t}(X_t) \mid Y_{0:t} = y_{0:t}, X_{t+1} = x_{t+1}] \\ &= \int T_{s|t}(x_t) \overleftarrow{\mathbf{Q}}_{\phi_t}(x_{t+1}, \mathrm{d}x_t) \\ &= \int T_{s|t}(x_t) \frac{q(x_t, x_{t+1})\phi_t(\mathrm{d}x_t)}{\int q(x'_t, x_{t+1})\phi_t(\mathrm{d}x'_t)}, \quad x_{t+1} \in \mathbf{X}. \end{aligned} \quad (5)$$

The recursion is initialised by setting

$$T_{s|s}(x_s) := h_s(x_s), \quad x_s \in \mathbf{X},$$

and for completeness we define

$$T_{s|u} \equiv 0 \text{ for } u < s.$$

By (3), $\phi_{s|t}h_s = \phi_t T_{s|t}$, and the target can hence be calculated by applying the filter ϕ_t to the function $T_{s|t}$.

Now the question arises when to stop updating the quantity of interest; indeed, since we are interested in computing the full vector (1) but opposed to letting the computational complexity of the algorithm increase with time, we are forced to terminate updating when the fluctuations of the sequence $\{\phi_t T_{s|t}\}_{t=s}^{\infty}$ have ceased. In the present paper we will stop updating at the time point s_ε for which the variance of $T_{s|t}$ under the filter ϕ_t falls below some given threshold $\varepsilon > 0$ for the first time. After that, we output $\phi_{s_\varepsilon} T_{s|s_\varepsilon}$ as our estimate of $\phi_{s|t}h_s$ for all $t \geq s_\varepsilon$. This choice can be clearly motivated by (5), from which it is clear that once $T_{s|t}$ is close to constant in the support of ϕ_t , then also $T_{s|t+1}$ is close to constant everywhere.

The algorithm can be summarized as follows.

- Initialise by letting $S \leftarrow \emptyset$. The set S will keep track of our active estimators. In addition, set the tolerance ε .
- For $t \leftarrow 0, 1, 2, 3, \dots$
 - for each $s \in S$, calculate $T_{s|t}(x_t)$ using (5);
 - let $S \leftarrow S \cup \{t\}$, i.e. activate an estimator at time t and set $T_{t|t} \leftarrow h_t$;
 - for each $s \in S$, calculate the variance $\mathbb{V}_{\phi_t}[T_{s|t}(X_t)]$; if it is smaller than ε , let $S \leftarrow S \setminus \{s\}$ and output $\phi_t T_{s|t}$.

B. Example: linear Gaussian SSMs

As mentioned previously, exact computation of the filter and joint-smoothing distributions is possible only for a few specific models. Here we present a Kalman-based version in the case of linear Gaussian SSMs.

In the linear Gaussian SSMs, an n_x -dimensional autoregressive state process is partially observed through n_y -dimensional observations. The model is specified by the equations

$$\begin{aligned} X_{t+1} &= AX_t + U_{t+1}, \\ Y_t &= BX_t + V_t, \end{aligned}$$

where $A \in \mathbb{R}^{n_x \times n_x}$ and $B \in \mathbb{R}^{n_y \times n_x}$ and $\{U_t\}_{t \in \mathbb{N}}$ and $\{V_t\}_{t \in \mathbb{N}}$ are sequences of mutually independent Gaussian

noises with zero mean and covariance matrices $\Sigma_U \in \mathbb{R}^{n_x \times n_x}$ and $\Sigma_V \in \mathbb{R}^{n_y \times n_y}$, respectively. All matrices are assumed to be pre-specified. Given the sequence $\{y_t\}_{t \in \mathbb{N}}$ of observations we wish to estimate (1) in the case of *affine* objective functions $h_s(x) = \alpha_s^\top x + \beta_s$, where $\alpha_s \in \mathbb{R}^{n_x}$ and $\beta_s \in \mathbb{R}$ are pre-specified.

In this model each filter ϕ_t is Gaussian, and the *Kalman filter* propagates its mean μ_t and covariance matrix Σ_t recursively through time. We calculate the backward kernel (2), which is proportional to the filter at time s times the transition density of the latent Markov chain. Since both these distributions are Gaussian with known mean and covariance matrices, it is easy to show that also the distribution of X_t conditioned on $X_{t+1} = x_{t+1}$ and $Y_{0:t} = y_{0:t}$ is Gaussian with mean $\mu_{t|t+1}(x_{t+1}) = \Sigma_{t|t+1}(A^\top \Sigma_U^{-1} x_{t+1} + \Sigma_t^{-1} \mu_t)$ and covariance matrix $\Sigma_{t|t+1} = (A^\top \Sigma_U^{-1} A + \Sigma_t^{-1})^{-1}$. We may hence write down a specific updating procedure for the functions $\{T_{s|t}\}_{t=s}^\infty$ in this case:

- Initialisation: for $t = s$, let $T_{s|s}(x_s) = h_s(x_s) = \alpha_s^\top x_s + \beta_s$.
- Proceeding recursively, assume that $\alpha_{s|t}$ and $\beta_{s|t}$ are of form $T_{s|t}(x_t) = \alpha_{s|t}^\top x_t + \beta_{s|t}$; then $T_{s|t+1}(x_{t+1}) = \alpha_{s|t+1}^\top x_{t+1} + \beta_{s|t+1}$, where

$$\begin{aligned} \alpha_{s|t+1}^\top &= \alpha_{s|t}^\top \Sigma_{t|t+1} A^\top \Sigma_U^{-1}, \\ \beta_{s|t+1} &= \alpha_{s|t}^\top \Sigma_{t|t+1} A^\top \Sigma_t^{-1} \mu_t + \beta_{s|t}. \end{aligned}$$

The last step of the algorithm—consisting in checking whether the variance of the function above is small enough—is now easily performed by calculating $\nabla_{\phi_t}[T_{s|t}(X_t)] = \alpha_{s|t}^\top \Sigma_t \alpha_{s|t}$ and comparing this with some pre-specified threshold ε . This completes all the steps needed for executing the algorithm, and we refer to Section VI for a numerical illustration.

Even though the previous method provides an exact implementation of the algorithm, it is limited to a single class of models and specific target functions. To move beyond this simplified setting we need to rely on approximations, and this will be discussed in the next section.

IV. PARTICLE-BASED ONLINE MARGINAL SMOOTHING

As mentioned previously, exact computation of the filter distributions—and hence the backward kernels—is possible only in a few specific cases. In the general case we will approximate these distributions using particle filters, which are recalled in the following.

A. Particle filters

A particle filter propagates recursively a set of particles with associated weights in order to approximate the filter distribution flow $\{\phi_t\}_{t \in \mathbb{N}}$ given the sequence $\{y_t\}_{t \in \mathbb{N}}$.

We describe recursively the most basic particle filter—the bootstrap filter [16]—and assume that we have at hand a sample $\{(\xi_t^i, \omega_t^i)\}_{i=1}^N$ of particles (the ξ_t^i) and associated weights (the ω_t^i) targeting the filter distribution ϕ_t in the sense that for all ϕ_t -integrable functions f ,

$$\sum_{i=1}^N \frac{\omega_t^i}{\Omega_t} f(\xi_t^i) \simeq \phi_t f,$$

where $\Omega_t := \sum_{i=1}^N \omega_t^i$ denotes the total weight and “ \simeq ” means that the estimator on the left hand side is *consistent*, i.e., converges in probability to the right hand side, as $N \rightarrow \infty$. To form a new weighted sample $\{(\omega_{t+1}^i, \xi_{t+1}^i)\}_{i=1}^N$ targeting the subsequent filter distribution ϕ_{t+1} , a two-step procedure is applied. First, the particles are resampled by drawing randomly a set of N independent indices $\{I_{t+1}^i\}_{i=1}^N$ from the categorical distribution induced by the probabilities proportional to the weights $\{\omega_t^i\}_{i=1}^N$, an operation denoted by $I_{t+1}^i \sim \text{Pr}(\{\omega_t^i\}_{i=1}^N)$, $i \in \{1, \dots, N\}$.

Second, the resampled particles are moved conditionally independently according to the dynamics of the state process, i.e., for all $i \in \{1, \dots, N\}$,

$$\xi_{t+1}^i \sim \mathbf{Q}(\xi_t^{I_{t+1}^i}, \cdot).$$

Finally, new importance weights are computed according to

$$\omega_{t+1}^i = g_{t+1}(\xi_{t+1}^i)$$

for all $i \in \{1, \dots, N\}$.

Initialisation is carried through by drawing $\xi_0^i \sim \chi$ and setting $\omega_0^i = g_0(\xi_0^i)$ for all $i \in \{1, \dots, N\}$.

We summarise the procedure in Algorithm 1, and denote by “ $\{(\xi_{t+1}^i, \omega_{t+1}^i)\}_{i=1}^N \leftarrow \text{PF}(\{(\xi_t^i, \omega_t^i)\}_{i=1}^N, y_{t+1})$ ” one application of Algorithm 1. (By convention we let $\{(\xi_0^i, \omega_0^i)\}_{i=1}^N \leftarrow \text{PF}(\{(\xi_{-1}^i, \omega_{-1}^i)\}_{i=1}^N, y_0)$ denote the initial step.)

Algorithm 1 Bootstrap particle filter

Require: A weighted sample $\{(\xi_t^i, \omega_t^i)\}_{i=1}^N$ targeting the filter distribution ϕ_t

- 1: **for** $i = 1 \rightarrow N$ **do**
 - 2: draw $I_{t+1}^i \sim \text{Pr}(\{\omega_t^\ell\}_{\ell=1}^N)$;
 - 3: draw $\xi_{t+1}^i \sim \mathbf{Q}(\xi_t^{I_{t+1}^i}, \cdot)$;
 - 4: set $\omega_{t+1}^i = g_{t+1}(\xi_{t+1}^i)$;
 - 5: **end for**
 - 6: **return** $\{(\xi_{t+1}^i, \omega_{t+1}^i)\}_{i=1}^N$
-

So far we have only considered estimation of the filter distributions. The rest of this section will be devoted to particle approximation of the marginal smoothing distributions.

For all $i \in \{1, \dots, N\}$, define recursively genealogical indices $\{G_{s|t}^i\}_{s=0}^t$ by $G_{t|t}^i = i$ and $G_{s-1|t}^i = I_s^{G_{s|t}^i}$. The set $\{(\xi_0^{G_{0|t}^i}, \dots, \xi_t^{G_{t|t}^i})\}_{i=1}^N$ is often referred to as the *genealogical tree* of the particles, and it is easy to show that the genealogical tree may, together with the importance weights $\{\omega_t^i\}_{i=1}^N$, be used for estimating the joint-smoothing distribution. In particular,

$$\sum_{i=1}^N \frac{\omega_t^i}{\Omega_t} h_s(\xi_s^{G_{s|t}^i}) \simeq \phi_{s|t} h_s, \quad (6)$$

which means a given marginal smoothing distribution $\phi_{s|t}$ can be approximated using the weighted sample formed by the *time s ancestors* of $\{\xi_t^i\}_{i=1}^N$. We refer to this estimator as the *Poor man’s smoother*. A well-known problem with the Poor man’s smoother is that the repeated resampling operations of the particle filter always deplete the genealogical tree in the

long run; thus, sooner or later, for some $s < t$ and some i_0 , $G_{u|t}^{i_0} = G_{u|t}^j$ for all $j \in \{1, \dots, N\}$ and all $u \in \{0, \dots, s\}$, implying that the estimates of $\phi_{u|t} h_u$, $u \in \{0, \dots, s\}$, will be based on only a single particle path. The work [18] establishes, under assumptions requiring typically the state space to be a compact set, a bound on the expected distance from the last generation to the most recent common ancestor that is proportional to $N \log(N)$ and *uniform* in time. Thus, the number of active, unique particles in the estimator (6) tends to one as t increases, leading to a depleted and impractical estimator.

B. Fixed-lag smoothing

To remedy the problem of particle lineage degeneracy, a fixed-lag smoother [22] can be used. The idea is to approximate the marginal smoothing distribution $\phi_{s|t}$ by the distribution $\phi_{s|s_\Delta(t)}$, where $s_\Delta(t) = (s + \Delta) \wedge t$ for some pre-specified lag $\Delta \in \mathbb{N}^*$. In this case, using the notation above, we get the biased approximation

$$\phi_{s|t} h_s \approx \sum_{i=1}^N \frac{\omega_{s_\Delta(t)}^i}{\Omega_{s_\Delta(t)}} h_s(\xi_s^{G_{s|s_\Delta(t)}^i}),$$

where $G_{s|s_\Delta(t)}^i$ is defined as above.

The approach requires suitable design of the lag Δ , and we face here a classical bias-variance tradeoff: if Δ is too small, then the forgetting of the model has not kicked in, and the discrepancy between the distributions is going to be large (leading to high bias); on the other hand, if Δ is too large, then, by path degeneracy, the estimate will be depleted (leading to high variance). The optimal choice of lag depends on the mixing of the SSM, and [27] proposes an optimal choice of Δ as $\lceil c \log(t) \rceil$, where the constant c depends on the mixing. This is problematic since it is hard to calculate, and even estimate, the mixing of an SSM. Thus, designing properly the lag is indeed a non-trivial task. The lag-based particle estimator that we propose in the next section relies again on forgetting-based arguments, but adapts the lag in a completely automatic manner.

C. The adaptive-lag smoother

We present here a particle-based version of the ideal algorithm in Section III-A, which can be thought of as an adaptive-lag smoother. In this algorithm we employ novel techniques for updating particle estimates of the functions $T_{s|t}$, and the adaptive lag can be thought of as the number of steps that each function is updated before the stopping criterion triggers truncation. The truncation depends heavily on the mixing of the model, but is now determined in an adaptive manner.

The critical step in the algorithm presented in Section III-A is the need of estimating and updating the statistics $T_{s|t}$ through the recursion (5). We proceed by induction and assume that we have at hand a set $\{\tilde{\tau}_{s|t}^i\}_{i=1}^N$ of estimates of $\{T_{s|t}(\xi_t^i)\}_{i=1}^N$. Proceeding as in [10], these estimates are

updated to estimates $\{\tilde{\tau}_{s|t+1}^i\}_{i=1}^N$ of $\{T_{s|t+1}(\xi_{t+1}^i)\}_{i=1}^N$ by replacing, in (5), ϕ_t by a particle approximation, yielding

$$\tilde{\tau}_{s|t+1}^i = \sum_{j=1}^N \frac{\omega_t^j q(\xi_t^j, \xi_{t+1}^i)}{\sum_{\ell=1}^N \omega_t^\ell q(\xi_t^\ell, \xi_{t+1}^i)} \tilde{\tau}_{s|t}^j, \quad i \in \{1, \dots, N\}, \quad (7)$$

where the ratio is a particle approximation of the backward kernel (2), and the particle approximation $\sum_{i=1}^N \omega_t^i \tilde{\tau}_{s|t}^i / \Omega_t \simeq \phi_{s|t} h_s$. Casting the recursion (7) into the ideal algorithm in Section III yields the following procedure:

- Initialise by letting $S \leftarrow \emptyset$ and setting the tolerance ε .
- For $t \leftarrow 0, 1, 2, 3, \dots$
 - run $\{(\xi_t^i, \omega_t^i)\}_{i=1}^N \leftarrow \text{PF}(\{(\xi_{t-1}^i, \omega_{t-1}^i)\}_{i=1}^N, y_t)$;
 - for each $s \in S$ and $i \in \{1, \dots, N\}$, calculate $\tilde{\tau}_{s|t}^i$ using (7);
 - let $S \leftarrow S \cup \{t\}$ and $\tilde{\tau}_{t|t}^i \leftarrow h_t(\xi_t^i)$ for all $i \in \{1, \dots, N\}$.
 - for each $s \in S$, if

$$\sum_{i=1}^N \frac{\omega_t^i}{\Omega_t} \left(\tilde{\tau}_{s|t}^i - \sum_{j=1}^N \frac{\omega_t^j}{\Omega_t} \tilde{\tau}_{s|t}^j \right)^2 < \varepsilon,$$

then let $S \leftarrow S \setminus \{s\}$ and output $\sum_{i=1}^N \omega_t^i \tilde{\tau}_{s|t}^i / \Omega_t$ as an estimate of $\phi_{s|t} h_s$ for all $t' \geq t$.

A drawback with the updating formula (7) is that it requires a sum of N terms to be computed for each particle, which yields an overall $\mathcal{O}(N^2)$ computational complexity. Needless to say, this is impractical when N is large.

To reduce the computational burden, we proceed as in the PaRIS [29, Alg. 2] and replace the right hand side of (7), which can be interpreted as an expectation, by a Monte Carlo estimate. More precisely, assuming that we have at hand a set $\{\tau_{s|t}^i\}_{i=1}^N$ of estimates of $\{T_{s|t}(\xi_t^i)\}_{i=1}^N$, we replace (7) by the mean

$$\tau_{s|t+1}^i = \frac{1}{\tilde{N}} \sum_{j=1}^{\tilde{N}} \tau_{s|t}^{J_t^{(i,j)}}, \quad (8)$$

where $\{J_t^{(i,j)}\}_{j=1}^{\tilde{N}}$ are conditionally independent draws from $\Pr(\{\omega_t^\ell q(\xi_t^\ell, \xi_{t+1}^i)\}_{\ell=1}^N)$ and \tilde{N} is a precision parameter. Such draws can most often be produced at low computational cost using rejection sampling. Indeed, assume that the transition density q is uniformly bounded by some constant $\bar{\varepsilon}$, i.e., $q(x, x') \leq \bar{\varepsilon}$ for all $(x, x') \in \mathcal{X}^2$; then, following [11], a draw J from $\Pr(\{\omega_t^\ell q(\xi_t^\ell, \xi_{t+1}^i)\}_{\ell=1}^N)$ can be produced by repeating the following steps until acceptance:

- (1) draw $J \sim \Pr(\{\omega_t^i\}_{i=1}^N)$;
- (2) accept J with probability $q(\xi_t^J, \xi_{t+1}^i) / \bar{\varepsilon}$.

Interestingly, under the mixing assumptions given in Section V it is possible to show that the expected number of trials required for sampling all the indices $\{J_t^{(i,j)}\}_{j=1}^{\tilde{N}}$ is linear in \tilde{N} ; see [29, Thm. 10]. This yields an $\mathcal{O}(N\tilde{N})$ algorithm, and as we will see below, \tilde{N} can be kept at a very low value (say, $\tilde{N} = 2$).

The variance of $T_{s|t}$ under ϕ_t is estimated using

$$\sigma_{s|t}^{2,N} := \sum_{i=1}^N \frac{\omega_t^i}{\Omega_t} \left(\tau_{s|t}^i - \sum_{\ell=1}^N \frac{\omega_t^\ell}{\Omega_t} \tau_{s|t}^\ell \right)^2,$$

and the updating procedure is stopped if $\sigma_{s|t}^{2,N} < \varepsilon$, where ε is some pre-chosen tolerance. Letting

$$s_\varepsilon^N(t) := \min\{u \geq s : \sigma_{s|u}^{2,N} < \varepsilon\} \wedge t, \quad (9)$$

we return the estimator

$$\phi_{s|t}^{N,\varepsilon} h_s := \sum_{i=1}^N \frac{\omega_{s_\varepsilon^N(t)}^i}{\Omega_{s_\varepsilon^N(t)}} \tau_{s|s_\varepsilon^N(t)}^i$$

of $\phi_{s|t} h_s$. The algorithm is presented in detail in Algorithm 2.

Algorithm 2 Adaptive-lag smoother

```

1: set  $S \leftarrow \{0\}$ ;
2: run  $\{(\xi_0^i, \omega_0^i)\}_{i=1}^N \leftarrow \text{PF}(\{(\xi_{-1}^i, \omega_{-1}^i)\}_{i=1}^N, y_0)$ ;
3: for  $i = 1 \rightarrow N$  do
4:   set  $\tau_{0|0}^i \leftarrow \tilde{h}_0(\xi_0^i)$ ;
5: end for
6: for  $t \leftarrow 1, 2, 3, \dots$  do
7:   run  $\{(\xi_t^i, \omega_t^i)\}_{i=1}^N \leftarrow \text{PF}(\{(\xi_{t-1}^i, \omega_{t-1}^i)\}_{i=1}^N, y_t)$ ;
8:   for  $i = 1 \rightarrow N$  do
9:     for  $j = 1 \rightarrow \tilde{N}$  do
10:      draw  $J_t^{(i,j)} \sim \text{Pr}(\{\omega_{t-1}^\ell q(\xi_{t-1}^\ell, \xi_t^i)\}_{\ell=1}^{\tilde{N}})$ ;
11:    end for
12:    for  $s \in S$  do
13:      set  $\tau_{s|t}^i \leftarrow \tilde{N}^{-1} \sum_{j=1}^{\tilde{N}} \tau_{s|t-1}^{J_t^{(i,j)}}$ ;
14:    end for
15:    set  $\tau_{t|t}^i \leftarrow h_t(\xi_t^i)$ ;
16:  end for
17:  set  $S \leftarrow S \cup \{t\}$ ;
18:  for  $s \in S$  do
19:    if  $\sigma_{s|t}^{2,N} < \varepsilon$  then
20:      set  $\phi_{s|t'}^{N,\varepsilon} h_s \leftarrow \sum_{i=1}^N \omega_t^i \tau_{s|t}^i / \Omega_t$  for all  $t' \geq t$ ;
21:      set  $S \leftarrow S \setminus \{s\}$ .
22:    end if
23:  end for
24: end for

```

Remark 2. In Algorithm 2 we let, on Line 7, the underlying particles be propagated by means of the standard bootstrap particle filter for simplicity. However, from a methodological point of view, running the proposed algorithm requires only access to a sequence of consistent samples—with or without weights—targeting the filter distribution flow, and it is, in practice, of subordinate importance how these samples are produced. This is relevant for, e.g., high-dimensional scenarios or scenarios with highly informative observations, where alternative particle filters, such as feedback particle filters [36] or auxiliary particle filters [30], may improve estimation significantly.

D. Designing algorithmic parameters

In Algorithm 2, the parameters ε and \tilde{N} are set by the user. Interestingly, [29] establishes that the PaRIS is (i) consistent for all fixed $\tilde{N} \in \mathbb{N}^*$ and (ii) numerically stable only if $\tilde{N} \geq 2$. The latter is illustrated by Figure 1, from which it is clear that using $\tilde{N} = 1$ leads to a degeneracy phenomenon that is reminiscent of the degeneracy of the genealogical tree. As it is

clear from the same figure, this phenomenon is avoided in the case $\tilde{N} = 2$. This distinction between the cases $\tilde{N} = 1$ and $\tilde{N} \geq 2$ is also present in the central limit theorem in [29, Thm. 8], where, in the marginal smoothing case, a time uniform $\mathcal{O}(1 + 1/\tilde{N})$ bound on the asymptotic variance is obtainable only in the case $\tilde{N} \geq 2$. As suggested by this bound, there is no gain in using a too large precision \tilde{N} , and typically $\tilde{N} = 2$ provides a satisfactory accuracy in simulations.

When it concerns the tolerance ε , using a smaller tolerance implies a larger lag, implying in turn more accurate estimates (and conversely). However, a larger lag requires a larger bank of active estimators, increasing in turn the computational time and memory requirement. This trade-off is studied in more detail in Section V and Section VI.

V. THEORY

A. Convergence of the sample variance criterion

We start off the theoretical analysis by studying the asymptotics (as $N \rightarrow \infty$) of the sample variances $\sigma_{s|t}^{2,N}$.

The analysis will be carried through under the following assumptions.

Assumption 1. For all $t \in \mathbb{N}$, $\|g_t\|_\infty < \infty$. Moreover, there exists a constant $|h|_\infty < \infty$ such that $\text{osc}(h_t) < |h|_\infty$ for all $t \in \mathbb{N}$.

Note that the first part of Assumption 1 implies finiteness of the particle weights. The following auxiliary result establishes the convergence of each sample variance criterion to a deterministic limit.

Lemma 3. Let Assumption 1 hold. Then for all $(s, t) \in \mathbb{N}^2$ such that $s \leq t$, it holds, as $N \rightarrow \infty$,

$$\sum_{i=1}^N \frac{\omega_t^i}{\Omega_t} \left(\tau_{s|t}^i - \sum_{\ell=1}^N \frac{\omega_t^\ell}{\Omega_t} \tau_{s|t}^\ell \right)^2 \xrightarrow{\mathbb{P}} \sigma_{s|t}^{2,\infty},$$

where

$$\sigma_{s|t}^{2,\infty} := \phi_t \{(T_{s|t} - \phi_t T_{s|t})^2\} + \eta_{s,t}$$

with $\eta_{s,t}$ being defined in Section A, Eqn. (11).

Second, we bound the limiting variance criterion. This calls for the following *strong mixing assumptions*.

Assumption 2.

- (i) There exist $0 < \underline{\varepsilon} < \bar{\varepsilon} < \infty$ such that $\underline{\varepsilon} < q(x, x') < \bar{\varepsilon}$ for all $(x, x') \in \mathcal{X}^2$.
- (ii) There exist $0 < \underline{\delta} < \bar{\delta} < \infty$ such that for all $t \in \mathbb{N}$, $\underline{\delta} < g_t(x) < \bar{\delta}$ for all $x \in \mathcal{X}$.

Under Assumption 2(i), define $\varrho := 1 - \underline{\varepsilon}/\bar{\varepsilon}$.

Assumptions similar to Assumption 2 are frequently in the literature (see, e.g., [8]) and require typically the state space of the hidden chain to be a compact set.

Theorem 4. Under Assumptions 1 and 2, it holds, for all $(s, t) \in \mathbb{N}^2$ such that $s \leq t$ and all $\tilde{N} \in \mathbb{N}^*$,

$$\sigma_{s|t}^{2,\infty} \leq |h|_\infty^2 \begin{cases} c_1 \varrho^{2(t-s)} + c_2 \tilde{N}^{-(t-s)} & \text{if } \tilde{N} \varrho^2 \neq 1, \\ \varrho^{2(t-s)} + c_3 (t-s) \tilde{N}^{-(t-s)} & \text{if } \tilde{N} \varrho^2 = 1, \end{cases} \quad (10)$$



Fig. 1. Genealogical traces corresponding to backward simulation in the adaptive-lag smoothing algorithm. Columns of nodes refer to different particle populations (with $N = 3$) at different time points (with time increasing rightward) and arrows indicate connections through the backward draws in the algorithm. The striped particles are in the final estimator for the marginal smoothing distribution when $s = 0$ and $t = 4$, black-colored particles are in the support of the historical trajectories of the final estimator, while gray-colored ones are inactive.

where the constants c_1, c_2 and c_3 are independent of s and t .

The first term in the bound (10) is related to the mixing of the SSM, and since $\varrho \in (0, 1)$ this term tends to zero geometrically fast as t grows. The second term is related to the Monte Carlo error induced by the PaRISian update. Here we clearly see that it is required that $\tilde{N} \geq 2$ in order for this term to vanish as t increases. In that case, $\sigma_{s|t}^{2,\infty} \rightarrow 0$ as $t \rightarrow \infty$.

B. Convergence of the estimator

In order to derive the asymptotic limit of our estimator we introduce the following notation. Let $s_\varepsilon(t) := \min\{u \geq s : \sigma_{s|u}^{2,\infty} < \varepsilon\} \wedge t$, which can be understood as the limit of $s_\varepsilon^N(t)$ (defined in (9)). In addition, let $\phi_{s|t}^\varepsilon := \phi_{s|s_\varepsilon(t)}$ and notice that this measure differs slightly from the adaptive-lag approximation delivered by the ideal algorithm in Section III-A, since the limiting variance $\sigma_{s|t}^{2,\infty}$ is not equal to $\mathbb{V}_{\phi_t}[T_{s|t}(X_t)]$; recall that the former also has an additional term $\eta_{s,t}$ corresponding to the Monte Carlo approximation of the backward kernel.

As expected and as established by the following theorem, $\phi_{s|t}^\varepsilon$ is indeed the asymptotic limit of the proposed estimator.

Theorem 5. *Let Assumptions 1 and 2 hold. Then for all $(s, t) \in \mathbb{N}^2$ such that $s \leq t$ and all bounded measurable functions h_s , as $N \rightarrow \infty$,*

$$\phi_{s|t}^{N,\varepsilon} h_s \xrightarrow{\mathbb{P}} \phi_{s|t}^\varepsilon h_s.$$

C. Bound on asymptotic memory requirement

Finally, we show that the memory requirement of the algorithm stays, in the asymptotic regime, uniformly bounded in t , which was a requirement in the problem statement. Asymptotically, the estimate of $\phi_{s|t} h_s$ is still under construction at time t if $\sigma_{s|t}^{2,\infty} \geq \varepsilon$ for all $t \in \{s, \dots, t\}$. Thus, let

$$\mathfrak{A}_t := \sum_{s=0}^t \prod_{u=s}^t \mathbb{1}_{\{\sigma_{s|u}^{2,\infty} \geq \varepsilon\}}$$

be the number of active adaptive-lag estimators at time t in the asymptotic regime.

Theorem 6. *Under Assumption 2, for all $\tilde{N} \geq 2$,*

$$\mathfrak{A}_t \leq \frac{\log(\varepsilon / \{ |h|_\infty^2 d(\varrho, \tilde{N}) \})}{\log(\varrho^2 \sqrt{\tilde{N}-1})},$$

where $d(\varrho, \tilde{N}) > 0$ depends on ϱ and \tilde{N} only.

We remark that the bound in Theorem 6 is uniform in time, implying a uniformly bounded memory requirement of the algorithm, at least in the asymptotic regime. Moreover, we note that the bound in Theorem 6 has an $\mathcal{O}(-\log \varepsilon)$ term.

VI. SIMULATIONS

We benchmark the algorithm on two different models. First we consider a linear Gaussian SSM, which enables computation of the exact distributions using the disturbance smoother Kalman smoother (see, e.g., [5, sec. 5.2.4]). The second model is the now classical stochastic volatility model proposed in [17].

A. Linear Gaussian SSM

Consider a linear Gaussian SSM given by the following set of equations:

$$\begin{aligned} X_{t+1} &= aX_t + \sigma_U U_{t+1}, \\ Y_t &= bX_t + \sigma_V V_t, \end{aligned}$$

where $\{U_t\}_{t \geq 0}$ and $\{V_t\}_{t \geq 0}$ are independent sequences of mutually independent standard Gaussian noise variables. Initially, $X_0 \sim \mathcal{N}(0, \sigma_V^2 / (1 - a^2))$. We consider smoothed means, corresponding to the objective functions $h_s = \text{id}$ for all $s \in \mathbb{N}$. We simulate a data record comprising 201 observations $y_{0:200}$ from the the model parameterised by $(a, b, \sigma_U, \sigma_V) = (.95, .5, .5, 2)$. Using tolerances $\varepsilon \in \{.5, .2, .1, 10^{-3}\}$ and $(N, \tilde{N}) = (400, 2)$ we performed 100 independent runs of the algorithm with the same input data. In addition, the Kalman version of the ideal algorithm (as presented in Section III-B) was run with the same tolerances as the particle version.

First, the estimates produced by these two algorithms are compared to exact values computed offline using the disturbance smoother. The outcome is displayed in Figure 2, from which it is clear that the estimates improve with decreasing tolerance. For $\varepsilon = .5$, the estimates exhibit clear fluctuations around the true values, while for $\varepsilon = 10^{-3}$ the estimates follow closely the true quantities. The top panel of Figure 3 reports time-averaged mean squared errors (MSEs) (with respect to the exact posterior means delivered by the disturbance smoother) for different values of ε . As expected, the MSE decreases monotonously with ε . However, since decreasing tolerance ε comes at the cost of computational work, we also introduce a measure of *efficiency*, defined as the product of reciprocal MSE and reciprocal CPU runtime. The bottom panel of Figure 3 reports efficiency for different values of ε . Since the bias of the

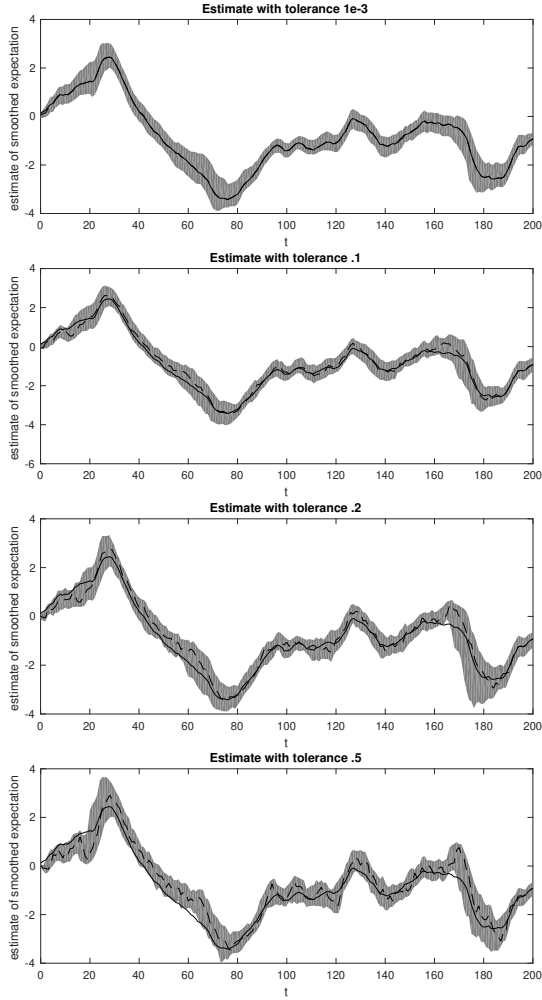


Fig. 2. Smoothed means for the linear Gaussian model. In each plot, the gray zone is the range of the particle-based estimates, while the black line indicates the exact smoothed values computed offline using the disturbance smoother. The dashed line is the Kalman version of our algorithm with the same tolerances as the particle-based method. When $\varepsilon = 10^{-3}$ the Kalman filter-based estimates and the exact values are more or less indistinguishable.

algorithm is more or less eliminated for all sufficiently small tolerances ε , there is an optimal value around $\varepsilon = .5 \times 10^{-3}$ for which the efficiency is maximal.

Finally, Figure 4 displays the initial variance criterion $\sigma_{0|t}^{2,N}$ for different values of t , and the plot is well in line with the exponentially decreasing bound provided by Theorem 4. Finally, we study the truncation lags $s_\varepsilon^N(t) - s$ determined by the algorithm for different tolerances. The average lags across the 100 runs are displayed in Figure 4, from which it is evident that decreasing ε leads, in accordance with Theorem 6, on the average to larger lags. The slope in the end of the plot indicates non-truncation.

B. Stochastic volatility model

The second model of consideration is the stochastic volatility model

$$\begin{aligned} X_{t+1} &= \phi X_t + \sigma U_{t+1}, \\ Y_t &= \beta \exp(X_t/2) V_t, \end{aligned}$$

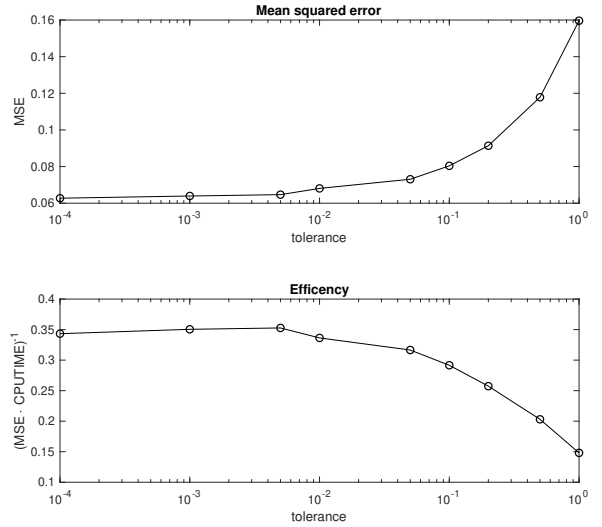


Fig. 3. Top panel: Time-averaged MSE for different tolerances ε . MSE decreases monotonously with ε . Bottom panel: Efficiency, defined as the product of reciprocal MSE and reciprocal CPU runtime, against tolerance ε . Maximal efficiency is reached for $\varepsilon = .5 \cdot 10^{-2}$.

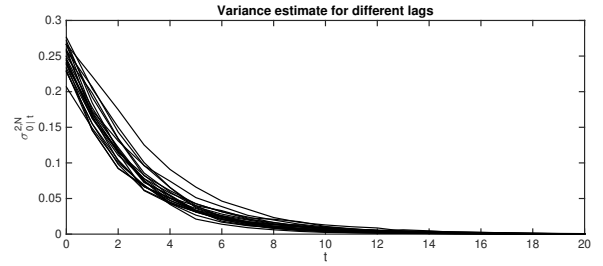


Fig. 4. Linear Gaussian model: the initial variance criterion $\sigma_{0|t}^{2,N}$ for different values of t .

where $\{U_t\}_{t \in \mathbb{N}}$ and $\{V_t\}_{t \in \mathbb{N}}$ are independent sequences of mutually independent standard Gaussian noise variables and $X_0 \sim \mathcal{N}(0, \sigma^2/(1 - \phi^2))$. In this nonlinear SSM, $\{Y_t\}_{t \in \mathbb{N}}$ can be thought of as the log-returns of a stock while $\{X_t\}_{t \in \mathbb{N}}$ can then be thought of as the unobserved log-volatility of the observed returns.

As before, we simulate 201 observations from the model indexed by $(\phi, \sigma, \beta) = (.98, \sqrt{.1}, \sqrt{.7})$. We employ the adaptive-lag smoother targeting again the mean of the marginal smoothing distribution, i.e., $h_s = \text{id}$ for all $s \in \mathbb{N}$. Algorithm 2 is run with the tolerances $\varepsilon \in \{.5, .1, 10^{-3}\}$ and sample sizes $(N, \tilde{N}) = (400, 2)$. The algorithm is executed 200 times for each value of ε , and all runs are based on the same data input. Since exact computation is infeasible for this

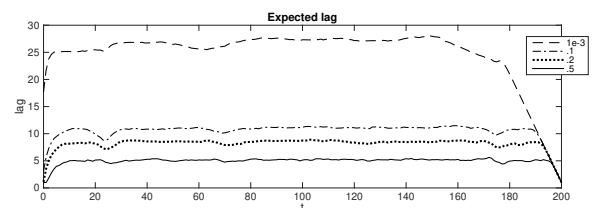


Fig. 5. Linear Gaussian model: average lag against time t .

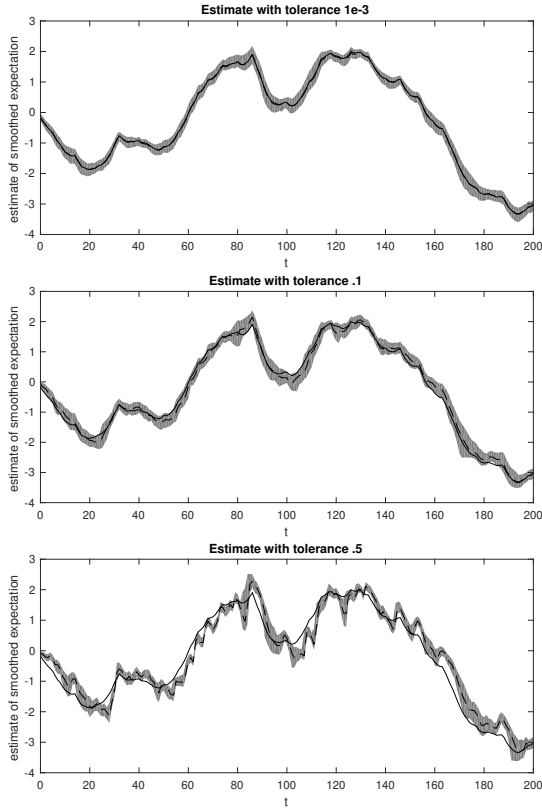


Fig. 6. Stochastic volatility model: smoothed means for different tolerances (cf. Figure 2).

nonlinear model, we use, as reference, proxies for the true posterior means obtained as the averages of 10 independent replicates of the full PaRIS (i.e., without stopping criterion) with $(N, \tilde{N}) = (2000, 2)$.

The outcome is reported in Figure 6. For $\varepsilon = .5$ the marginal smoothing estimates of the adaptive-lag smoother deviate significantly from the ground truth of the PaRIS algorithm for most time-steps. Decreasing the tolerance to $\varepsilon = .1$ yields clearly improved—but still undesirably volatile—estimates. However, decreasing the tolerance even further to $\varepsilon = 10^{-3}$ leads to a plot where the PaRIS estimates are firmly in the area of the estimates produced by the adaptive-lag smoother, and taking the mean over all the adaptive-lag estimates yields values indistinguishable from the estimates delivered by the PaRIS.

Finally, Figure 7 provides the average lags at different time steps, and obviously the nonlinear components of the model leads to a higher degree of adaptation compared to the linear Gaussian model.

C. Comparison with fixed-lag smoothing

We end the numerical illustrations with a comparison of the adaptive-lag smoother to the fixed-lag smoother. As mentioned earlier, in the fixed-lag smoother a lag has to be set a priori. The determination of the optimal lag requires the user to make a complex bias-variance tradeoff, governed by the mixing properties of the model as well as the coalescence properties of the particle paths. It is hence impossible to determine

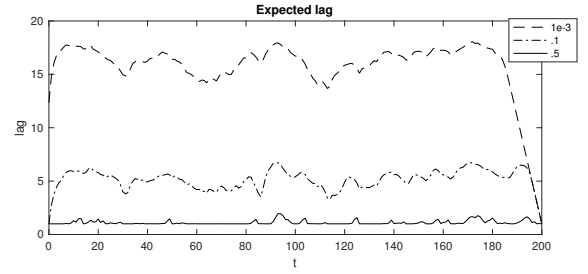


Fig. 7. Stochastic volatility model: average lags for different tolerances.

the optimal lag without first carrying through a preparatory simulation study. We simulate new data from both the linear Gaussian and the stochastic volatility models using the same parameters as above and compare the adaptive-lag approach with $\varepsilon \in \{.5, .2, .1, 10^{-3}, 10^{-6}\}$ and $(N, \tilde{N}) = (400, 2)$ to the fixed-lag approach with lags $\Delta \in \{1, 2, 4, 8, 16, 32, 64, 128\}$ and $N = 400$. For both models we simulate 1001 observations and aim at estimating $\mathbb{E}[X_s^2 \mid Y_{0:1000}]$. We perform 200 independent runs of all algorithms. The results are displayed in Figure 8, where we have chosen $s = 750$ for illustration. From the plot it is clear that too small choices of the lag Δ lead to significant bias, while too large choices increase excessively the variance. The optimal choice of Δ can be seen to be somewhere around $\Delta = 8$ and $\Delta = 16$ for both models in this example. On the other hand, from the same plot it is clear that the tolerance ε does not obey the same bias-variance-tradeoff. When ε is simply small enough, the adaptive-lag smoother provides estimates having a variance being on par with that of the optimally tuned fixed-lag smoother. Moreover, importantly, decreasing excessively to $\varepsilon = 10^{-6}$ does not, by the numerical stability of the PaRIS-type smoothing estimates, imply additional variance.

VII. CONCLUSION

In this paper we have presented a novel algorithm—an adaptive-lag marginal smoother—for online computation of marginal-smoothing expectations in general SSMs. We are not aware of any other algorithm in the literature solving satisfactorily this challenging problem.

The proposed algorithm differs from the standard particle-based fixed-lag smoother [22], [27] (in our view, the only competitor of the proposed method) in essentially two ways: first, the estimates produced by the algorithm do not at all suffer from particle path degeneracy; second, the lag is designed adaptively by the algorithm via a variance criterion. Remarkably, since the PaRIS-type updates stabilize completely the support of the estimator as long as $\tilde{N} \geq 2$, the user does not risk afflicting the produced estimates with undesired variance by using an unnecessarily small tolerance ε and, consequently, an unnecessarily large average lag. This is the main advantage of the proposed algorithm over particle-based fixed-lag smoothing.

We remark that the proposed algorithm is, just like the PaRIS, *function specific* in the sense that it is adjusted to the given sequence $\{h_t\}_{t \in \mathbb{N}}$ of objective functions and outputs directly a sequence of estimated expectations rather than a

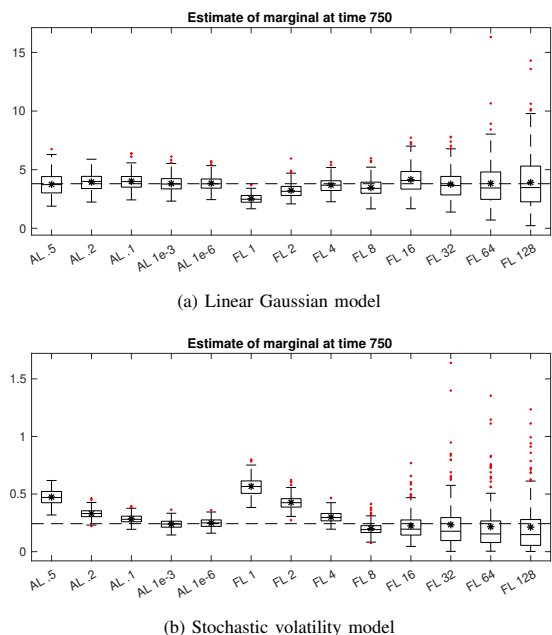


Fig. 8. Comparison of the adaptive-lag smoother and the fixed-lag smoother for the linear Gaussian model (a) and stochastic volatility model (b). The black stars indicate the sample mean for each algorithm and the dashed line indicates a ground truth calculated exactly by the Kalman smoother in (a) and with the PaRIS algorithm in (b).

sequence of weighted samples targeting the marginal smoothing distributions of interest. Thus, solving the problem (1) for *different* objective function sequences requires different function-specific updates (8) to be run in parallel. Still, nothing prevents these updates to be based on the same underlying particle filter and even the same backward draws $J_t^{(i,j)}$.

Like all existing particle-based forward-filtering backward-smoothing-type algorithms, the proposed procedure relies on particle approximation of the backward kernels. Such approximation requires typically the SSM to be fully dominated. Even though many SSMs used in practice are indeed fully dominated, extending the methodology beyond this class of models is an important direction of research. Moreover, in our work we linearize the computational complexity of the backward sampling operation—the computational bottleneck of the algorithm—using the accept-reject approach proposed in [11]. However, in practice, especially when the state space X is high dimensional, the upper bound $\bar{\varepsilon}$ may be very large, implying only a limited computational gain. In such cases, the adaptive-stopping approach suggested in [34] may come in useful. Finally, as in all backward-sampling-type smoothing algorithms, problems may occur for models and observation sequences for which the filter and smoothing distributions have significantly different support; we refer to [33] for a discussion.

When it concerns the theoretical developments, a result that is missing in the present paper is a rigorous theoretical analysis of the estimator’s bias and the dependence of the bias on the tolerance ε . Since the estimator is driven by ergodicity arguments, such an analysis requires control of the forgetting of the backward chain. However, this is still an open—and

presumably very complex—problem, and the question is thus left as future research.

Needless to say, the strong mixing assumptions (see Assumption 2) driving the theoretical analysis of our estimator are restrictive. Still, these are standard in the literature, and only a few—technically involved—works analyze the time-uniform convergence of particle filters under weaker, verifiable assumptions that can be checked also for nonlinear SSMs with non-compact state space; see e.g. [35], [12]. When it concerns particle-based backward smoothing, [19] provides a stochastic stability analysis of the FFBSm algorithm under assumptions that point to applications with non-compact state spaces, and a similar approach may be applicable to our estimator.

The convergence results presented in Section V hold only asymptotically as $N \rightarrow \infty$, and to furnish the estimator with error bounds for finite N would be appealing. When it concerns the PaRIS, it is indeed possible to derive an exponential concentration inequality for fixed N (see [29, Corollary 2]), and we thus expect such a Hoeffding-type bound to hold also for the estimator proposed in the present paper. However, to derive a *time uniform* exponential concentration inequality for these algorithms appears to be considerably more complicated, as Hoeffding’s inequality, which would be the first tool to try out in the proof, seems to be too crude for this purpose. Hence, we also have to leave this as future work.

ACKNOWLEDGMENT

The authors would like to thank the anonymous referees for insightful comments that improved the presentation of the paper. The work of J. Olsson is supported by the Swedish Research Council, Grant 2018-05230.

REFERENCES

- [1] B. D. O. Anderson and J. B. Moore. *Optimal Filtering*. Prentice-Hall, 1979.
- [2] C. Andrieu, A. Doucet, and R. Holenstein. Particle Markov chain Monte Carlo methods. *Journal of the Royal Statistical Society. Series B (Statistical Methodology)*, 72(3):269–342, 2010.
- [3] M. Briers, A. Doucet, and S. Maskell. Smoothing algorithms for state-space models. *Annals Institute Statistical Mathematics*, 62(1):61–89, 2010.
- [4] O. Cappé. Online EM algorithm for hidden Markov models. *Journal of Computational and Graphical Statistics*, 20(3):728–749, 2011.
- [5] O. Cappé, E. Moulines, and T. Rydén. *Inference in Hidden Markov Models*. Springer, 2005.
- [6] S. Chib, F. Nadari, and N. Shephard. Markov chain Monte Carlo methods for stochastic volatility models. *J. Econometrics*, 108:281–316, 2002.
- [7] P. De Jong. A cross validation filter for time series models. *Biometrika*, 75:594–600, 1988.
- [8] P. Del Moral. *Feynman-Kac Formulae. Genealogical and Interacting Particle Systems with Applications*. Springer, 2004.
- [9] P. Del Moral, A. Doucet, and S. Singh. A Backward Particle Interpretation of Feynman-Kac Formulae. *ESAIM M2AN*, 44(5):947–975, 2010.
- [10] P. Del Moral, A. Doucet, and S. Singh. Forward smoothing using sequential Monte Carlo. Technical report, Cambridge University, 2010.
- [11] R. Douc, A. Garivier, E. Moulines, and J. Olsson. Sequential Monte Carlo smoothing for general state space hidden Markov models. *Ann. Appl. Probab.*, 21(6):2109–2145, 2011.
- [12] R. Douc, E. Moulines, and J. Olsson. Long-term stability of sequential Monte Carlo methods under verifiable conditions. *Ann. Appl. Probab.*, 24(5):1767–1802, 2014.
- [13] A. Doucet, S. Godsill, and C. Andrieu. On sequential Monte-Carlo sampling methods for Bayesian filtering. *Stat. Comput.*, 10:197–208, 2000.

- [14] P. Fearnhead, D. Wyncoll, and J. Tawn. A sequential smoothing algorithm with linear computational cost. *Biometrika*, 97(2):447–464, 2010.
- [15] S. J. Godsill, A. Doucet, and M. West. Monte Carlo smoothing for non-linear time series. *J. Am. Statist. Assoc.*, 50:438–449, 2004.
- [16] N. Gordon, D. Salmond, and A. F. Smith. Novel approach to nonlinear/non-Gaussian Bayesian state estimation. *IEE Proc. F, Radar Signal Process.*, 140:107–113, 1993.
- [17] J. Hull and A. White. The pricing of options on assets with stochastic volatilities. *J. Finance*, 42:281–300, 1987.
- [18] P. E. Jacob, L. M. Murray, and S. Rubenthaler. Path storage in the particle filter. *Statistics and Computing*, pages 1–10, 2013.
- [19] A. Jasra. On the behaviour of the backward interpretation of Feynman-Kac formulae under verifiable conditions. *Journal of Applied Probability*, 52(2):339–359, 2015.
- [20] S. J. Julier and J. K. Uhlmann. A new extension of the Kalman filter to nonlinear systems. In *AeroSense: The 11th International Symposium on Aerospace/Defense Sensing, Simulation and Controls*, 1997.
- [21] G. Kitagawa. Monte-Carlo filter and smoother for non-Gaussian nonlinear state space models. *J. Comput. Graph. Statist.*, 1:1–25, 1996.
- [22] G. Kitagawa and S. Sato. Monte Carlo smoothing and self-organising state-space model. In *Sequential Monte Carlo methods in practice*, Stat. Eng. Inf. Sci., pages 177–195. Springer, New York, 2001.
- [23] F. Lindsten, P. Bunch, S. J. Godsill, and T. B. Schön. Rao-blackwellized particle smoothers for mixed linear/nonlinear state-space models. In *2013 IEEE International Conference on Acoustics, Speech and Signal Processing*, pages 6288–6292, May 2013.
- [24] L. Mihaylova, D. Angelova, S. Honary, D. R. Bull, C. N. Canagarajah, and B. Ristic. Mobility tracking in cellular networks using particle filtering. *IEEE Transactions on Wireless Communications*, 6(10):3589–3599, 2007.
- [25] G. Mongillo and S. Denève. Online learning with hidden Markov models. *Neural Computation*, 20(7):1706–1716, 2008.
- [26] Thi Ngoc Minh Nguyen, Sylvain Le Corff, and Eric Moulines. On the two-filter approximations of marginal smoothing distributions in general state-space models. *Advances in Applied Probability*, 50(1):154177, 2017.
- [27] J. Olsson, O. Cappé, R. Douc, and E. Moulines. Sequential Monte Carlo smoothing with application to parameter estimation in non-linear state space models. *Bernoulli*, 14(1):155–179, 2008. arXiv:math.ST/0609514.
- [28] J. Olsson and J. Westerborn. Efficient particle-based online smoothing in general hidden Markov models. In *IEEE 2014 International Conference on Acoustics, Speech, and Signal Processing (ICASSP 2014)*, 2014.
- [29] J. Olsson and J. Westerborn. Efficient particle-based online smoothing in general hidden markov models: The PaRIS algorithm. *Bernoulli*, 23(3):1951–1996, 2017.
- [30] M. K. Pitt and N. Shephard. Filtering via simulation: Auxiliary particle filters. *J. Am. Statist. Assoc.*, 94(446):590–599, 1999.
- [31] L. R. Rabiner. A tutorial on hidden Markov models and selected applications in speech recognition. *Proc. IEEE*, 77(2):257–285, 1989.
- [32] L. R. Rabiner and B-H. Juang. *Fundamentals of Speech Recognition*. Prentice-Hall, 1993.
- [33] H.-C. Ruiz and H. J. Kappen. Particle smoothing for hidden diffusion processes: Adaptive path integral smoother. *IEEE Transactions on Signal Processing*, 65:3191–3202, 2017.
- [34] E. Taghavi, F. Lindsten, L. Svensson, and T. Schön. Adaptive stopping for fast particle smoothing. *Proceedings of the 38th International Conference on Acoustics, Speech, and Signal Processing (ICASSP)*, pages 6293–6297, 2013.
- [35] R. van Handel. Uniform time average consistency of Monte Carlo particle filters. *Stochastic Processes and their Applications*, 119(11):3835–3861, 2009.
- [36] T. Yang, P. G. Mehta, and S. P. Meyn. Feedback particle filter. *IEEE Transactions on Automatic Control*, 58(10):2465–2480, Oct 2013.

APPENDIX

We preface the proofs by some additional notation.

For all $t \in \mathbb{N}$, define the unnormalised transition kernels

$$\mathbf{L}_t(x_t, dx_{t+1}) := g_{t+1}(x_{t+1}) \mathbf{Q}(x_t, dx_{t+1}),$$

with the convention that $\mathbf{L}_s \mathbf{L}_t \equiv \text{id}$ when $s > t$. In addition, we let $\mathbf{L}_{-1}(x, dx_0) := g_0(x_0) \delta_x(dx_0)$. Moreover, we may

express each joint smoothing distribution $\phi_{0:t|t}$ as $\phi_{0:t|t} = \phi_t \mathbf{T}_t$, where we have defined the kernels

$$\mathbf{T}_t(x_t, dx_{0:t-1}) := \begin{cases} \prod_{s=0}^{t-1} \overleftarrow{\mathbf{Q}}_{\phi_s}(x_{s+1}, dx_s) & \text{for } t \in \mathbb{N}^*, \\ \text{id} & \text{for } t = 0. \end{cases}$$

Notice that $T_{s|t}(x_s)$ in (4) can be expressed as $T_{s|t}(x_s) = \mathbf{T}_t h_s(x_s)$. Finally, define the operator

$$\mathbf{D}_t : h \mapsto \mathbf{T}_t(h - \phi_{0:t|t}h),$$

acting on the space of bounded measurable functions.

Proof of Lemma 3. By [29, Lemma 13] it holds that

$$\sum_{i=1}^N \frac{\omega_t^i}{\Omega_t} (r_{s|t}^i)^2 \xrightarrow{\mathbb{P}} \phi_t(\mathbf{T}_t^2 h_s) + \eta_t,$$

where

$$\eta_t := \sum_{\ell=s}^{t-1} \tilde{N}^{\ell-t} \frac{\phi_\ell \mathbf{L}_\ell \{ \overleftarrow{\mathbf{Q}}_{\phi_\ell}(\mathbf{T}_\ell h_s - \mathbf{T}_{\ell+1} h_s)^2 \mathbf{L}_{\ell+1} \cdots \mathbf{L}_{t-1} \mathbb{1}_X \}}{\phi_\ell \mathbf{L}_\ell \cdots \mathbf{L}_{t-1} \mathbb{1}_X}. \quad (11)$$

In addition, from [29, Theorem 1] we get that

$$(\phi_{s|t}^N h_s)^2 \xrightarrow{\mathbb{P}} \phi_t^2(\mathbf{T}_t h_s),$$

and combining the previous two limits yields, as $N \rightarrow \infty$,

$$\begin{aligned} \sigma_{s|t}^{2,N} &= \sum_{i=1}^N \frac{\omega_t^i}{\Omega_t} (r_{s|t}^i)^2 - \left(\sum_{i=1}^N \frac{\omega_t^i}{\Omega_t} r_{s|t}^i \right)^2 \\ &\xrightarrow{\mathbb{P}} \sigma_{s|t}^{2,\infty} := \phi_t(\mathbf{T}_t^2 h_s) - \phi_t^2(\mathbf{T}_t h_s) + \eta_t \\ &= \phi_t \{ (\mathbf{T}_t h_s - \phi_t \mathbf{T}_t h_s)^2 \} + \eta_t. \end{aligned} \quad (12)$$

□

Proof of Theorem 4. We begin by noticing that

$$\phi_t \{ (\mathbf{T}_t h_s - \phi_t \mathbf{T}_t h_s)^2 \} = \phi_t(\mathbf{D}_t^2 h_s).$$

Thus, by [11, Lemma 10] it holds, for all $t \geq s$,

$$\|\mathbf{D}_t h_s\|_\infty \leq \varrho^{t-s} |h|_\infty,$$

giving us the bound

$$\|\phi_t(\mathbf{D}_t^2 h_s)\|_\infty \leq \varrho^{2(t-s)} |h|_\infty^2$$

on the first term of (12). In order to bound the second term of (12), i.e. η_t , we note that, [11, Lemma 10] yields that

$$\|\mathbf{T}_\ell h_s - \mathbf{T}_{\ell+1} h_s\|_\infty \leq 2\varrho^{\ell-s} |h|_\infty.$$

In addition, under Assumption 2, for all $x \in X$,

$$\begin{aligned} &\underline{\varepsilon} \mu(g_{\ell+2} \mathbf{L}_{\ell+2} \cdots \mathbf{L}_{t-1} \mathbb{1}_X) \\ &\leq \mathbf{L}_{\ell+1} \cdots \mathbf{L}_{t-1} \mathbb{1}_X(x) \leq \\ &\bar{\varepsilon} \mu(g_{\ell+2} \mathbf{L}_{\ell+2} \cdots \mathbf{L}_{t-1} \mathbb{1}_X). \end{aligned}$$

Combining the previous two bounds allows η_t to be bounded; indeed, proceed like

$$\begin{aligned} & \frac{\phi_\ell \mathbf{L}_\ell \{ \overleftarrow{\mathbf{Q}}_{\phi_\ell} (\mathbf{T}_\ell h_s - \mathbf{T}_{\ell+1} h_s)^2 \mathbf{L}_{\ell+1} \cdots \mathbf{L}_{t-1} \mathbf{1}_X \}}{\phi_\ell \mathbf{L}_\ell \cdots \mathbf{L}_{t-1} \mathbf{1}_X} \\ & \leq 4 \varrho^{2(\ell-s)} |h|_\infty^2 \frac{\varepsilon}{\underline{\varepsilon}} = \varrho^{2(t-s)} \frac{4|h|_\infty^2}{(1-\varrho)}. \end{aligned}$$

Assuming now that $\tilde{N}\varrho^2 \neq 1$ we may bound η_t using that

$$\begin{aligned} \eta_t & \leq \frac{4|h|_\infty^2}{(1-\varrho)} \sum_{\ell=s}^{t-1} \tilde{N}^{\ell-t} \varrho^{2(\ell-s)} \\ & = \frac{4|h|_\infty^2}{(1-\varrho)} \tilde{N}^{-t} \varrho^{-2s} \sum_{\ell=s}^{t-1} (\tilde{N}\varrho^2)^\ell \\ & = \frac{4|h|_\infty^2}{(1-\varrho)(1-\tilde{N}\varrho^2)} \left(\tilde{N}^{-(t-s)} - \varrho^{2(t-s)} \right). \end{aligned} \quad (13)$$

On the other hand, if $\tilde{N}\varrho^2 = 1$, (13) yields

$$\eta_t \leq \frac{4|h|_\infty^2}{(1-\varrho)} \tilde{N}^{-(t-s)} (t-s).$$

The previous argument may be summarised as

$$\sigma_{s|t}^{2,\infty} \leq |h|_\infty^2 \begin{cases} c_1 \varrho^{2(t-s)} + c_2 \tilde{N}^{-(t-s)} & \text{if } \tilde{N}\varrho^2 \neq 1, \\ \varrho^{2(t-s)} + c_3 (t-s) \tilde{N}^{-(t-s)} & \text{if } \tilde{N}\varrho^2 = 1, \end{cases}$$

where

$$c_1 := 1 - \frac{4}{(1-\varrho)(1-N\varrho^2)}, \quad c_2 := \frac{4}{(1-\varrho)(1-N\varrho^2)}, \quad c_3 := \frac{4}{(1-\varrho)}.$$

□

Proof of Theorem 5. Write

$$\begin{aligned} \phi_{s|t}^{N,\varepsilon} h_s & = \sum_{u=s+1}^t \mathbf{1}_{\{s_\varepsilon^N(t)=u\}} \phi_{s|u}^N h_s \\ & = \sum_{u=s+1}^t \phi_{s|u}^N h_s \mathbf{1}_{\{\sigma_{s|u}^{2,N} < \varepsilon\}} \prod_{\ell=s+1}^{u-1} \mathbf{1}_{\{\sigma_{s|\ell}^{2,N} \geq \varepsilon\}} \\ & \quad + \phi_{s|t}^N h_s \prod_{\ell=s+1}^t \mathbf{1}_{\{\sigma_{s|\ell}^{2,N} \geq \varepsilon\}}. \end{aligned}$$

By Lemma 3 and Theorem 4 it holds that $\sigma_{s|t}^{2,N} \xrightarrow{\mathbb{P}} \sigma_{s|t}^{2,\infty}$ as $N \rightarrow \infty$. This yields, by Slutsky's theorem, as $N \rightarrow \infty$,

$$\begin{aligned} \phi_{s|t}^{N,\varepsilon} h_s & \xrightarrow{\mathbb{P}} \sum_{u=s+1}^t \phi_{s|u} h_s \mathbf{1}_{\{\sigma_{s|u}^{2,\infty} < \varepsilon\}} \prod_{\ell=s+1}^{u-1} \mathbf{1}_{\{\sigma_{s|\ell}^{2,\infty} \geq \varepsilon\}} \\ & \quad + \phi_{s|t} h_s \prod_{\ell=s+1}^t \mathbf{1}_{\{\sigma_{s|\ell}^{2,\infty} \geq \varepsilon\}} = \sum_{u=s+1}^t \mathbf{1}_{\{u=s_\varepsilon(t)\}} \phi_{s|u} h_s. \end{aligned}$$

□

Proof of Theorem 6. Note that

$$\mathfrak{A}_t = \sum_{s=0}^t \prod_{u=s}^t \mathbf{1}_{\{\sigma_{s|u}^{2,\infty} \geq \varepsilon\}} \leq \sum_{s=0}^t \mathbf{1}_{\{\sigma_{s|t}^{2,\infty} \geq \varepsilon\}}.$$

Now, we consider separately the two cases $\tilde{N}\varrho^2 \neq 1$ and $\tilde{N}\varrho^2 = 1$.

First, assume that $\tilde{N}\varrho^2 \neq 1$.

By Theorem 4, $\sigma_{s|t}^{2,\infty} \geq \varepsilon$ implies that $|h|_\infty^2 c_1 \varrho^{2(t-s)} + |h|_\infty^2 c_2 \tilde{N}^{-(t-s)} \geq \varepsilon$. To proceed further, consider the two sub-cases (i): $\tilde{N}^{-1} > \varrho^2$ and (ii): $\tilde{N}^{-1} < \varrho^2$.

(i) In this case, $c_1 < 0$; thus, if

$$|h|_\infty^2 c_1 \varrho^{2(t-s)} + |h|_\infty^2 c_2 \tilde{N}^{-(t-s)} \geq \varepsilon,$$

then

$$|h|_\infty^2 c_2 \tilde{N}^{-(t-s)} \geq \varepsilon.$$

Consequently, an upper limit on $(t-s)$ is given by

$$(t-s) \leq \frac{\log(\varepsilon/\{|h|_\infty^2 c_2\})}{\log \tilde{N}^{-1}}.$$

Thus, \mathfrak{A}_t may be bounded according to

$$\begin{aligned} \mathfrak{A}_t & \leq \sum_{s=0}^t \mathbf{1}_{\left\{ (t-s) \leq \frac{\log(\varepsilon/\{|h|_\infty^2 c_2\})}{\log \tilde{N}^{-1}} \right\}} \\ & \leq \frac{\log(\varepsilon/\{|h|_\infty^2 c_2\})}{\log \tilde{N}^{-1}}. \end{aligned}$$

(ii) In this case, $c_2 < 0$; thus, as previously,

$$(t-s) \leq \frac{\log(\varepsilon/\{|h|_\infty^2 c_1\})}{\log \varrho^2},$$

yielding the bound

$$\mathfrak{A}_t \leq \frac{\log(\varepsilon/\{|h|_\infty^2 c_1\})}{\log \varrho^2}.$$

We now assume that $\tilde{N}\varrho^2 = 1$. In this case, $\sigma_{s|t}^{2,\infty} \geq \varepsilon$ implies that $|h|_\infty^2 \tilde{N}^{-(t-s)} \{1 + c_3(t-s)\} \geq \varepsilon$ as c_3 is always positive and $t \geq s$. Thus,

$$(t-s) \leq \frac{\log(\varepsilon/\{|h|_\infty^2 (1+c_3)\})}{\log \tilde{N}^{-1}}.$$

providing the bound

$$\mathfrak{A}_t \leq \frac{\log(\varepsilon/\{|h|_\infty^2 (1+c_3)\})}{\log \tilde{N}^{-1}}.$$

Combining these results gives us the final bound

$$\mathfrak{A}_t \leq \frac{\log(\varepsilon/\{|h|_\infty^2 d(\varrho, \tilde{N})\})}{\log(\varrho^2 \sqrt{\tilde{N}^{-1}})}$$

for a constant $d(\varrho, \tilde{N})$ depending on the constants c_1, c_2 , and c_3 as well as the values of ϱ^2 and \tilde{N} . □